Earthquakes and Structures, *Vol. 11, No. 2 (2016) 195-215*
DOI: http://dx.doi.org/10.12989/eas.2016.11.2.195

Practical seismic assessment of unreinforced masonry historical buildings

Stylianos I. Pardalopoulos[*1,2], Stavroula J. Pantazopoulou[1,3a] and Christos E. Ignatakis[4b]

[1]*Department of Civil and Environmental Engineering, University of Cyprus, Nicosia, Cyprus*
[2]*Institute of Engineering Seismology and Earthquake Engineering, Thessaloniki, Greece*
[3]*Department of Civil Engineering, Lassonde Faculty of Engineering, York University, Canada*
[4]*Department of Civil Engineering, Aristotle University of Thessaloniki, Thessaloniki, Greece*

(Received October 9, 2015, Revised June 25, 2016, Accepted July 12, 2016)

Abstract. Rehabilitation of historical unreinforced masonry (URM) buildings is a priority in many parts of the world, since those buildings are a living part of history and a testament of human achievement of the era of their construction. Many of these buildings are still operational; comprising brittle materials with no reinforcements, with spatially distributed mass and stiffness, they are not encompassed by current seismic assessment procedures that have been developed for other structural types. To facilitate the difficult task of selecting a proper rehabilitation strategy - often restricted by international treaties for non-invasiveness and reversibility of the intervention - and given the practical requirements for the buildings' intended reuse, this paper presents a practical procedure for assessment of seismic demands of URM buildings - mainly historical constructions that lack a well-defined diaphragm action. A key ingredient of the method is approximation of the spatial shape of lateral translation, Φ, that the building assumes when subjected to a uniform field of lateral acceleration. Using Φ as a 3-D shape function, the dynamic response of the system is evaluated, using the concepts of SDOF approximation of continuous systems. This enables determination of the envelope of the developed deformations and the tendency for deformation and damage localization throughout the examined building for a given design earthquake scenario. Deformation demands are specified in terms of relative drift ratios referring to the in-plane and the out-of-plane seismic response of the building's structural elements. Drift ratio demands are compared with drift capacities associated with predefined performance limits. The accuracy of the introduced procedure is evaluated through (a) comparison of the response profiles with those obtained from detailed time-history dynamic analysis using a suite of ten strong ground motion records, five of which with near-field characteristics, and (b) evaluation of the performance assessment results with observations reported in reconnaissance reports of the field performance of two neoclassical torsionally-sensitive historical buildings, located in Thessaloniki, Greece, which survived a major earthquake in the past.

Keywords: seismic assessment; historical and monumental buildings; unreinforced masonry structures (URM); pushover analysis; torsion

*Corresponding author, Ph.D., E-mail: stylpard@gmail.com
[a]Professor, E-mail: pantaz@ucy.ac.cy, pantazo@yorku.ca
[b]Professor, E-mail: ignatak@civil.auth.gr

http://www.techno-press.com/journals/eas&subpage=7 ISSN: 2092-7614 (Print), 2092-7622 (Online)

1. Introduction

Load-bearing unreinforced masonry (URM) buildings built during and after the Renaissance up to the early 20th century attract an emerging interest for their preservation through rehabilitation and retrofit. Having a lifetime ranging between one to more than five centuries, URM construction encompasses a vast variety of structures, ranging from residential heritage buildings to monumental edifices built to house government or state activities (Fig. 1). These buildings are a living part of history, defining the ambiance of the cities to which they belong and at the same time being operational in several cases, housing modern day uses.

Being influenced by the conceptual design principles that prevailed during and after the Renaissance, URM historical construction possess special dynamic characteristics that lead to a certain pattern of response during an earthquake excitation. To achieve the desired harmony, which was inspired from highly regarded classical forms, architects of the era designed buildings that were characterized by symmetry in plan and in height, loaded with architectural elements inspired from archaic forms (for example colonnades, reliefs in gables, and carefully chosen aspect ratios). In single-unit buildings, the structure was designed in plan so as to have a simple geometrical shape, rectangular or prismatic. Multi-unit buildings were designed to have a system-plan organized along a main axis of symmetry, whereas in many cases a transversal axis of symmetry in plan also exists. To achieve plan symmetry, building volumes were often organized in the form of an **E**, an **H**, an **L**, a **Π** or a **T**, with courtyards located in the recesses of these shapes so that the overall plan could be thought to form a concave prism, whereas at each building-wing long corridors usually span from one end of the building volume to the other (Fig. 2). In every case, side views of the building were designed to have windows and doors symmetrically spaced with respect to a vertical axis that was intersecting the plan symmetry axis, whereas the area occupied by openings (i.e., windows and doors) was gradually increased from the ground level to the top of the building (resulting to the corresponding reduction in the area of walls).

These design principles are responsible for the systematic development of certain types of structural damages in buildings of this category located in countries of high seismicity, such as countries of the Mediterranean basin. This is especially evident in cases of multi-volume, monumental URM buildings, where in many cases of uniaxial symmetry the plan arrangement is responsible for the development of in-plan torsional phenomena during a seismic excitation in direction orthogonal to the axis of symmetry. Torsion in plan can cause significant damage at locations of the building that are remote relative to the center of twist of the complex building plan. This is why structural damages are frequently reported in post-earthquake reconnaissance

Fig. 1 Heritage buildings of the 19th and 20th century in Nafplio and Thessaloniki, Greece

reports of monumental URM buildings, occurring mainly at the court recesses, where separate building volumes are joined, as well as at the walls of corridors with significant length between successive transverse walls, owing to dynamic displacements in the out-of-plane direction (Fig. 2).

The residual strength of historical and monumental URM buildings is reduced from a vague undetermined value, which would represent the initial state. A starting estimate of residual strength, on which to benchmark the effectiveness of upgrading retrofit measures, is often obtained through Finite Element analysis of idealized models of the current state of the structure. However, despite the sophistication of modern computing software platforms, the obtained results are not necessarily dependable when applied to this class of structures, owing to inherent limitations of the numerical analysis algorithms (Pardalopoulos *et al*. 2015, Pantazopoulou 2013). This is mainly because (a) URM is brittle and unreinforced, presenting intense post-peak softening in the response envelope of pier members immediately after cracking. This is detrimental to the ability of standard algorithms to reach convergence and avoid numerical instability. (b) Most of the available commercial software today used in seismic assessment do not offer the option of 3-D analysis with nonlinear shell elements that are needed in order to model masonry wall behavior and (c) They also do not offer complete options for nonlinear dynamic response estimations, except for combinations of modal response maxima, which, being based on the principle of superposition, precludes the option for even considering secondary sources of nonlinearity (e.g., contact interface opening). Additional restrictions result from modern seismic codes (EC8-3 2005) that prohibit application of sophisticated analyses procedures in buildings where material and geometric properties are classified at a limited "knowledge level"; this is the typical case with URM historical buildings (knowledge level is quantified by codes according with strict, prescribed procedures and is used to control permissible analyses that may be employed in order to establish demand as well as the associated safety factors).

As a result, conducting seismic assessment of historic buildings and monuments by utilizing procedures that were originally developed and tailored to the properties of modern frame structures can result in underestimation of the residual strength of the corresponding structure. Underestimating the available strength could lead to rather invasive choices of rehabilitation methods, contrary to the spirit of international treaties for noninvasiveness and reversibility of the intervention (ICOMOS 1964), that can alter or destroy the unique historical or architectural

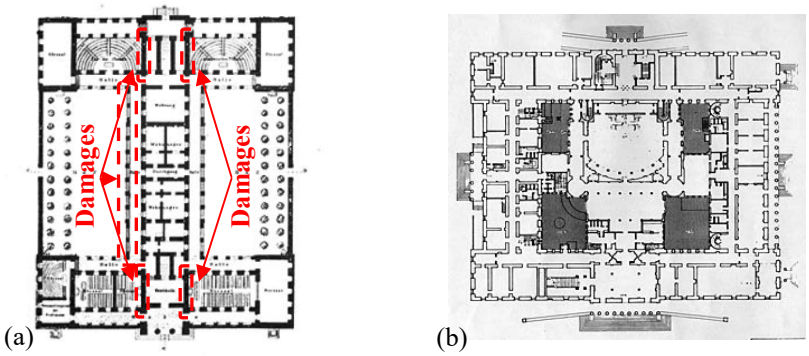

Fig. 2 Plans of monumental buildings located in Athens, Greece (http://www.eie.gr/archaeologia/En/Index.aspx.): (a) the University of Athens Central Building (1864) (locations of developed damages during the 1999 Athens earthquake), (b) The Hellenic parliament (1847)

features of the building in the interest of perceived needs for strength increase of the structure. To address this problem a number of researchers have recently been investigating alternative methods for representation of the mechanical properties of masonry (Roca *et al.* 2010) and variations of assessment procedures, suitable for the simulation and the assessment of URM historical buildings (Giresini *et al.* 2015, Illampas *et al*. 2014, Bracchi *et al*. 2015, Psycharis *et al*. 2013, Borzi *et al*. 2008). Also conducted were large scale research projects on the establishment of new performance-based assessment procedures for this category of structures (D' Ayala and Lagomarsino 2015).

2. Rapid seismic assessment of URM buildings

In light of all the difficulties encountered in the endeavor of seismic assessment of URM buildings, a palatable alternative that would also be consistent with the limitations owing to the "knowledge limitation" is required. Towards this idea it would be useful to borrow as many elements as is consistent with first principles from the Code-established simplified seismic assessment methods for engineered buildings (where mass is located primarily at floor levels). These are the following:

(I) Describe the seismic hazard in spectral format: smoothed expressions relate the structural total acceleration, $S_a(T)$ of a linear elastic, single degree of freedom (SDOF) system with the peak ground acceleration, a_g, through the system's period T.

(II) Idealize the structure as an Equivalent SDOF system. In practical Seismic Design it is customary to consider the structure as a generalized SDOF system vibrating only in its fundamental mode of behavior, T_1. So, spectral acceleration represents the total acceleration response of the structure, given by the spectrum at T_1, i.e., $S_a(T_1)$; Spectral displacement at T_1 is estimated from $S_a(T_1)$ from the product, $S_d=S_a(T_1)\cdot T_1^2/(2\cdot\pi)^2\approx S_a(T_1)\cdot(T_1^2/40)$. This spectral displacement response is converted to actual building response, after multiplication with the excitation factor, $\Gamma\,(=[\Phi^T\cdot m\cdot r]/[\Phi^T\cdot m\cdot\Phi])$, where m is the mass matrix of the structure, Φ the fundamental response mode, and r a vector of influence coefficients (Clough and Penzien 1976). The displacements result from application of the seismic force on the building, which is quantified by the base shear $V_a(=m^*\cdot S_a(T_1))$, ($m^*=[\Phi^T\cdot m\cdot r]^2/[\Phi^T\cdot m\cdot\Phi]$ is the effective mass of the structure in the mode considered, otherwise expressed as $\lambda\cdot W/g$). Usually $\Gamma>1$, and $\lambda<1$, but the product $\Gamma\cdot\lambda\approx1$. For continuous systems, λ is seldom over 0.6 for the first translational mode, whereas the corresponding Γ value may be as high as 1.8 or more (ATC 40, 1996). To keep things simple EN 1998-1 (2004) allows using the value of 1 for both coefficients for up to two storey buildings, when combined with static analysis using the code design spectra.

(III) Calculate inelastic seismic demands from the elastic response estimation through pertinent q-μ-T relationships (EN 1998-1 2004). This requires first estimation of the required q factor, from the ratio $q=V_a/V_y$, where V_y is the estimated base shear strength of the building. An example regarding these relationships is available in EN 1998-1 (2004), according to which

$$\mu = q \;\; for \;\; T_1 > T_C \;\; ; \quad \mu = 1 + (q-1)\cdot\frac{T_C}{T} \;\; for \;\; T_1 < T_C \tag{1}$$

(IV) Localize the displacement demands after multiplication of the building displacement with the fundamental mode shape, Φ. Thus, the displacement at any point with coordinates (x_i, y_i, z_i) is

obtained as, $\Delta_i = \Gamma \cdot S_d(T_1) \cdot \Phi(x_i,y_i,z_i)$.

To apply the above steps to a URM building the following additional open issues need to be resolved:

(a) The fundamental mode of response may not easily be determined for this class of buildings through classical Finite Element Analysis. It appears that due to the spatial continuity of mass and stiffness occurring in URM buildings (mass is distributed in the vertical walls rather than the floor levels), combined with the frequent lack of stiff diaphragms, an unusual phenomenon occurs, probably of purely numerical origin, where modes with the highest periods often concern the isolated vibration of secondary flexible components (such as lone timber beam in the floor that mobilizes an insignificant modal mass, or a room divider) overwhelming the actual translational mode of vibration of the entire building. In general, very small mass participation occurs in several closely spaced modes, in a density that is entirely related to the density and detail of the mesh, to the extent that one would need to include several tens or hundreds of modes in order to engage even 65% of the building mass, with no clearly identifiable predominant response mode in these numerical models of the structure.

(b) Since calculation of inelastic response is precluded with the current state of the art, unless the building may be idealized as a conventional frame (this has been done but a pre-requisite assumption is the availability of stiff diaphragms, see Kouris and Kappos 2015, Lagomarsino *et al*. 2013), one needs to make assumptions regarding the q-μ-T relationships that would be applicable for this class of structures; but experimental data is too limited to support a departure from the general framework which is established by codes of practice for all types of buildings in general, so Eq. (1) will be used in the remainder.

To overcome the difficulties associated with estimation of a translational mode that could be used in the ESDOF idealization of the building, concepts from approximate vibration analysis are used, according to which, the shape function in the Rayleigh quotient that yields the lowest vibration frequency is the normalized shape assumed by the structure when it is loaded in the direction of the earthquake by its own distributed weight (Clough and Penzien 1976, Chapter 9); thus, it is the nearest approximation to the fundamental vibration mode. This idea is extended in the present approach to the complex continuous spatial system of a URM building. It is easy to perform lateral load analysis for the spatially distributed self weight of the structure, provided that the gravitational field is taken to act in the direction of the earthquake (i.e., laterally, rather than in the vertical direction of the structure). By so doing, all the mass is engaged in inertia force equal to the self weight. The structure deflects as a cantilever, having the building plan in the role of a cross section. Walls oriented orthogonally to the applied lateral acceleration deform in out-of-plane action, whereas walls oriented parallel to the applied acceleration deform in in-plane flexure and shear action. The deflected shape thus obtained, is subsequently normalized with respect to the displacement of a selected reference point, referred to hereon as the control node; locating the control node at the center of gravity of the floor plan is ideal, as it allows the use of a rough empirical approximation in the value of Γ, without requiring detailed calculation. Note however that in principle, any point can be used as a reference for normalization, according to the concepts of generalized SDOF systems (Clough and Penzien 1976, Chapter 2).

The normalized shape of lateral deflection thus obtained, is a dependable approximation of the shape assumed by the structure during random excitation, such as the earthquake motion. The shape, denoted henceforth by Φ, is a continuous function in space, following the continuous nature of the structural envelope. Being a continuous function, its gradients, or deviation, between successive points quantify deformation; thus, the shape function, which is calculated according to

the preceding approximate analysis, is endowed with significant information about the areas of compliance where deformation is expected to localize, and depending on the deformation capacity of the region, it signifies the areas where damage may be anticipated.

Shape function Φ mobilizes the highest possible fraction of the building's total mass in the corresponding direction of excitation (i.e., more than 50%, which is very high as compared to the normal mode shapes obtained after solution of eigenvalue analysis). For a given earthquake scenario the proposed assessment procedure for URM structures uses Φ in order to convert global seismic demands to local deformation demands - which is essential for evaluation of the expected performance. From previous investigations of the characteristics of $\Phi(x,y,z)$ in actual URM structures, it has been shown that this response shape is an adequate approximation of the response envelopes obtained from time history analysis at peak response, while requiring significantly less effort and shorter computational time (Pardalopoulos *et al*. 2015, Pardalopoulos and Pantazopoulou 2015). The procedure consists of the following two practical steps:

Step 1 - Determination of the envelope of the developed deformations of the examined building during seismic excitation: A three-dimensional finite element model of the building is subjected to a notional gravitational field that acts horizontally in each of the two principal plan directions of the building and then is analyzed statically. Taking into consideration the brittle response of URM, which cannot secure a positive definite stiffness of pier members after cracking, the examined building is simulated as a linear finite element model allowing only for localized points of non-linear response at contact points in order to avoid numerical instabilities. To capture both in-plane and out-of-plane actions, basic element unit in the discretization of the piers and spandrels is a typical thick shell with elastic properties. Each static analysis provides a three-dimensional deflected shape of the examined building, which, after normalizing to the average displacement of the plan centroid of the crest of the building, may be considered a lateral response shape function. This shape function is denoted henceforth as $\Phi(x,y,z)$. The fundamental translational period of the structure is estimated using the following empirical relationship

$$T_1 = 0.050 \cdot H^{3/4} \tag{2}$$

where, H is the total building height, in (m), measured from the level of foundation or the level of rigid basement. Next, the total acceleration and relative displacement demands are estimated from the design response spectra, for the region where the building is located (a_{gR} is the reference value of design peak ground acceleration on type A ground); for usual building heights, the period T_1 calculated according to Eq. (2) is lower that the value T_C at the end of the constant acceleration range of the design spectrum

$$S_a(T_1) = \gamma_I \cdot a_{gR} \cdot S \cdot 2.5 \;\; ; \;\; S_d(T_1) = S_a(T_1) \cdot \left(\frac{T_1}{2 \cdot \pi} \right)^2 \approx S_a(T_1) \cdot T_1^2 / 40 \,, \;\; S_d(T_1) \le S_a(T_C) \cdot T_C^2 / 40 \tag{3}$$

In the above, γ_I is the building's importance factor, and S is the soil factor. Using the shape function and the ESDOF response estimation, the displacement envelope throughout the structure is approximated from Displacements and Rotations (relative drift ratio, θ, between two points i, j of the building envelope)

$$\Delta(x,y,z) = \Gamma \cdot S_d(T_1) \cdot \Phi(x,y,z) \;\; ; \;\; \theta_{i,j} = \Gamma \cdot S_d(T_1) \cdot \frac{\Phi(x_j,y_j,z_j) - \Phi(x_i,y_i,z_i)}{L_{i,j}} \tag{4}$$

where $L_{i,j}$ is the distance between the points considered (drift ratios are meaningful indices of deformation and damage).

Step 2 - Determination of local seismic demand and application of acceptance criteria: The bearing capacity in URM historical structures can be best identified by the amount of deformation that may be sustained by the structural components. Deformation demand is a more meaningful index than force demand in seismic assessment of building behavior; note that according to the literature, the equal displacement rule is valid even in an approximate sense - that is, elastic displacement demands are close to the inelastic ones. However, it is not as easily justifiable to claim an analogous relationship between the forces calculated from inelastic and elastic analyses (Muto *et al*. 1960, Newmark *et al*. 1973). In the framework of the introduced simple seismic assessment procedure, local seismic demand is specified in terms of relative drift ratios, referring to the in-plane relative deviation of the piers' and walls' ends from vertical, θ_{in}, and to URM facades deviating from the horizontal initial orientation in out-of-plane deflection, θ_{out}. The relative drift ratio in plane, θ_{in}, is defined as the horizontal relative displacement (i.e., the difference) that occurs between two points along the building height, (i.e., ends of a pier or a wall), divided by their vertical distance. Similarly, θ_{out} is defined as the outwards relative deflection between successive points in the building plan, divided by their horizontal distance. Meaningful indices include the relative displacement between the midspan and corners of walls oriented normal to the direction of seismic action, which quantify the intensity of out-of-plane action; also the relative displacement at the end points of wings relative to the main structure, which indicate the tendency for torsional response, θ_{tor}. These may be examined at the floor levels and at the crest of the building. Definitions of θ_{in}, θ_{out} and θ_{tor} are presented in Fig. 3. Thus, the fraction of the θ_{in} value, which is owing to the torsional response, is equal to $\theta_{tor} \cdot L/H$, where L is the length of wing from the point of support and H the height of the structure at the point considered.

The values of θ_{in}, θ_{out} and θ_{tor} calculated above are then compared to the corresponding performance levels imposed by the seismic code applicable at the site. Cracking rotations (drift ratios) in masonry elements, θ_y, are in the order of 0.15% for in-plane and 0.20% for out-of-plane wall deformation (corresponding to the *Operational/Immediate Occupancy* limit state). EN1998-1 (2004) (Eurocode 8-3 for seismic assessment of existing structures) specifies in Chapter 9 that for masonry buildings values of relative drift ratios that vary between θ_y and $3/4 \cdot \theta_u$, correspond to *Significant but Repairable Damage* performance level, whereas for higher values of θ_{in} and θ_{out}, ranging up to the limit of $4/3 \cdot \theta_u$, damage occurring to the structural elements is classified as *Life-Safe/No collapse* performance level. The ultimate drift capacity, θ_u, according to the same code,

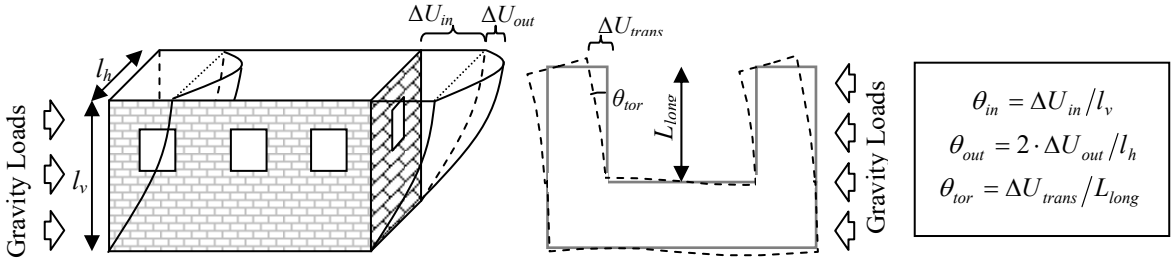

Fig. 3 Definition of relative drift ratios θ_{in}, θ_{out} and θ_{tor} (subscripts refer to in-plane, out-of-plane and torsional action)

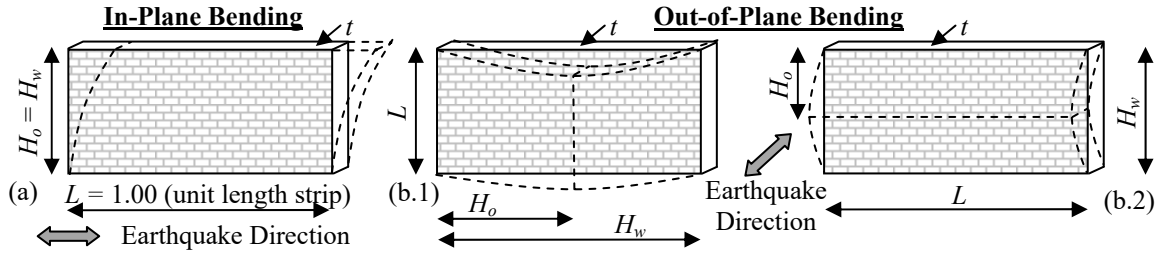

Fig. 4 Definitions of H_o, H_w and L for the cases of (a) in-plane deformation (b) out-of-plane wall bending

depends on the mode of failure controlling the response (i.e., whether flexural or shear strength has the least value). In in-plane shear, flexural and shear strengths of a wall are estimated from

$$V_y = \min\{V_f, V_s\}, \text{ where, } V_f = \frac{L \cdot N}{2 \cdot H_o} \cdot \left(1 - 1.15 \cdot \frac{N}{L \cdot t \cdot f_d}\right) \; ; \; V_s = 0.4 \cdot N < 0.065 \cdot f_b \cdot L' \cdot t \quad (5)$$

The dimension of the element's cross section normal to the axis of bending is the cross section's length, L, whereas t is the thickness, $f_d=f_m/CF_m$, f_m is the mean compressive strength of mortar and CF_m (=1.35, 1.20 and 1.00) is the confidence factor according to EC8-3 (2005) related to the knowledge level of the geometric and material properties of examined building. L' denotes the depth of the wall cross section that is under net normal compression when considering the sum of the gravity load stresses and the flexural moments due to the earthquake. Drift capacity for in-plane wall response is

$$\text{Walls controlled by Flexure:} \quad \theta_u = 0.008 \cdot H_o / L \quad (6a)$$

$$\text{Walls controlled by Shear:} \quad \theta_u = 0.004 \quad (6b)$$

On the other hand, the out-of-plane drift capacity is limited by flexure and by toppling of the wall during rocking response, as follows

$$\theta_u = \min\{\theta_{u,1}, \theta_{u,2}\} \quad (7)$$

where, $\theta_{u,1}=0.003 \cdot H_o/t$ is the flexural rotation capacity, and $\theta_{u,2}=\theta_{R,u} \cdot (1-M_y/M_{Rd})$ is the rocking limit. Eqs. (6)-(7) apply both to the wall piers and spandrels, or complete panels. Auxiliary terms in Eq. (7) are defined as follows: $\theta_{R,u}=t/H_o$ is the rigid body rotation before the wall becomes unstable and topples (this happens when the restoring force, which here is the axial load of the wall, goes through the pole of rotation at the base, Griffith *et al*. 2003). Parameter $M_y=(f_{wt}+(N/(L \cdot t))) \cdot (L \cdot t^2)/6$ is the cracking moment of the wall, where f_{wt} is the tensile strength of the masonry material and H_o is the distance between poles of rotation of the wall during rocking motion. In the out-of-plane motion (Fig. 4(b), (c)), the flexural demand, M_{Rd}, corresponds to the moment created by an assumed uniform pressure acting on the wall surface, owing to inertia of the distributed wall mass to acceleration. The resultant of this pressure is, $F_{Rd}=S_a(T_1) \cdot t \cdot \gamma \cdot A_{L,w}$ and $A_{L,w}=L \cdot H_w - A_{op}$, where H_w is the total wall height (Fig. 4) and A_{op} is the total area of openings along the examined wall. Therefore, $M_{Rd}=F_{Rd} \cdot H_o/2$.

3. Investigation of seismic response of torsionally-vulnerable URM historical buildings

To demonstrate the proposed procedure in practical assessment of seismic response of historic URM buildings, two, torsionally sensitive, neoclassical buildings have been simulated as three-dimensional finite element models and subjected to a series of time-history dynamic analyses, according to a suite of strong ground motions. These buildings were constructed in the end of the 19th century in Thessaloniki, Greece and during their service life they have sustained numerous seismic excitations, which caused damages of different degree in their structural systems. Yet, even after more than a century of service life, they still remain in good condition and are ideal case studies for evaluating the accuracy of the proposed procedure for seismic assessment of this class of URM buildings.

3.1 Description of the buildings

The first building is the *Papafeion Foundation*, depicted in Fig. 5. Operating continuously since 1903 as a boarding school, the building is a three storey neoclassical edifice, consisting of three building wings, which, in plan form the shape of the capital letter **E**.

The entire building complex is enclosed within a rectangle of external dimensions of 81.50×55.44 m, whereas the building height (excluding the height of the timber roof) is 15.03 m (heights of the three storeys: 3.60 m, 5.65 m, 5.78 m) except for the central wing, where the corresponding height is 17.83 m due to an elevation of the roof of the building's ceremonial hall (Fig. 5(e)). The first-storey walls are made of stone, 0.80 m thick in the perimeter of the building and 0.70 m in the inner plan. Second storey walls comprise solid bricks, whereas third storey walls are made of voided bricks. Perimeter walls are 0.55 m thick, whereas internal walls are 0.40 m

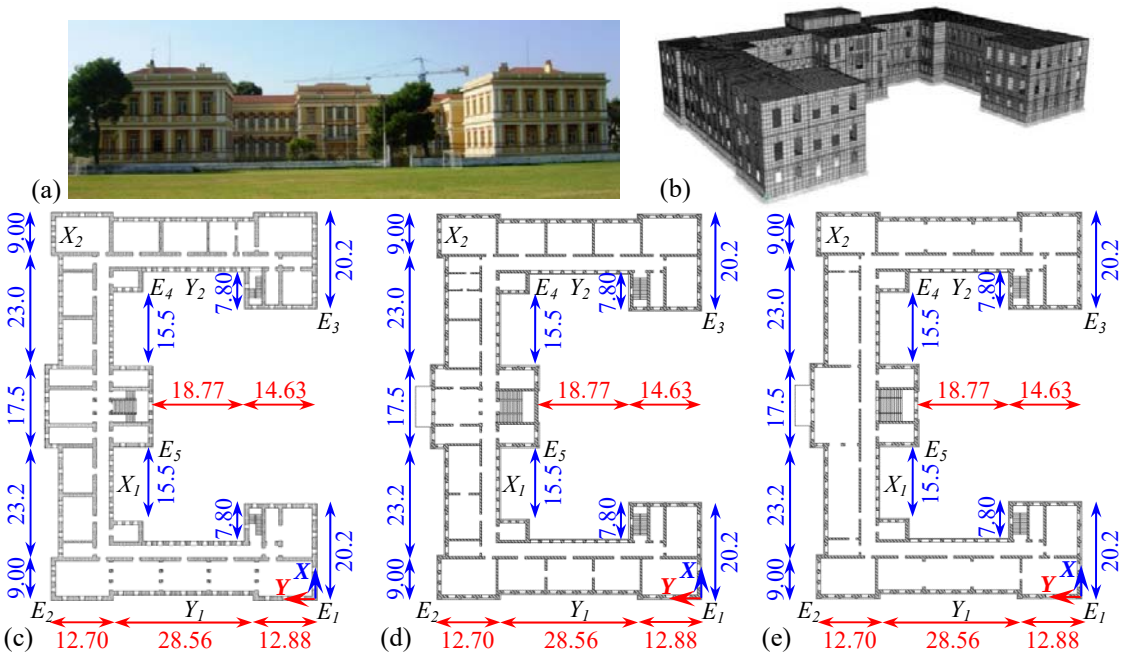

Fig. 5 The Papafeio Foundation: (a) North view, (b) 3D finite element building model, (c - e) 1st, 2nd and 3rd storey plan views, respectively

thick, in both storeys. Floors of the first and the second storey are made of double T iron beams, having a 0.1×0.18 m and a 0.08×0.18 m cross section at each storey, respectively, spanning the smaller room dimensions, while in corridors the spacing is 0.65 m in the first and 0.67 m in the second storey. The roof of the third storey is also made of double T iron beams, oriented similarly to the iron beams of the 1st and the 2nd storey floors, having a cross section of 0.08×0.2 m and a spacing of 0.85 m. Brick-arches, spanning in the transverse direction between successive iron beams, are encased between the upper and lower flanges of the double T beams, in all floors (Fig. 6(d)). The total thickness of the building's horizontal structural elements (including the finishing) at the location of the iron beams is 0.34 and 0.30 m in the first and second storey floor and 0.20 m in third storey roof, whereas the thickness at the highest point of the arches is smaller by about 0.10 m. The last storey is covered by a roof made of timber, trusses spanning along the longitudinal dimensions of the building's wings, yet this roof is not part of the structural system of the building.

The second building is a conventional two-storey neoclassical building with a basement and a timber roof (Fig. 6(a)). It was built in 1895 and during its service life it housed different functions, last serving as the 12th primary school of Thessaloniki. The building has a 15.25×15.25 m square plan, whereas a rectangular 5.6×6.1 m in-plan extension in its North-East corner houses auxiliary functions. The total building height, without its timber roof, is 12 m (storey heights: basement

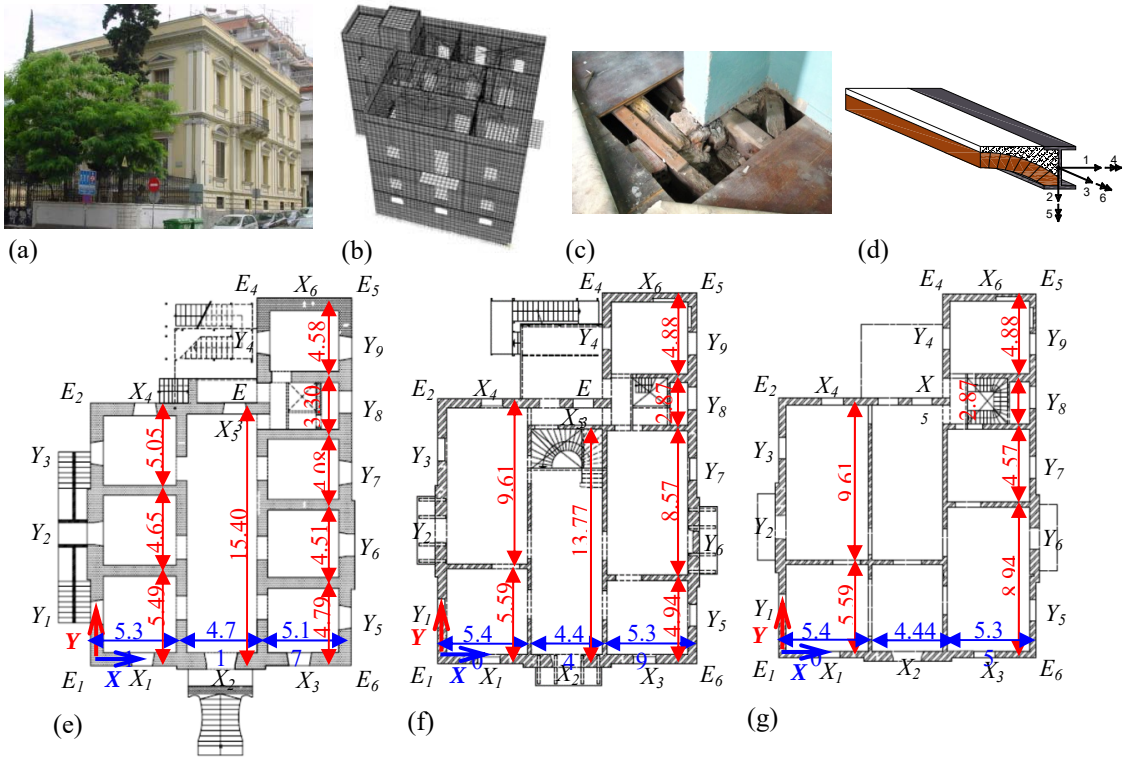

Fig. 6 The 12th Primary School of Thessaloniki: (a) South-East view, (b) 3D finite element building model, (c - d) construction details of timber floors and of floor with iron beams filled with brick arches, respectively, (e - g) basement, 1st and 2nd storey plan views, respectively

2.7 m, 1st storey 4.4 m, 2nd storey 4.9 m). The main part of the building is covered by a square, timber-framed roof, whereas, the roof of the building's rectangular extension is formed as terrace. Access to the terrace is achieved via a rectangular, 2.3 m height penthouse. The basement walls are made of stone, being 0.7 m thick in the perimeter, 0.9 m thick in the central sections of the East, West and South facades (locations denoted as Y_6, Y_2 and X_2, respectively, in Fig. 6(c)-(e)) and 0.6 m thick in the building's interior. Walls of the 1st and 2nd storey comprise solid brick, following the layout of the basement walls. First storey walls are 0.46 m thick in the perimeter, 0.7 m thick at locations Y_6, Y_2 and X_2 in Fig. 6 and 0.23 m thick in the interior of the building, whereas the corresponding wall thickness at the building's second storey are 0.34 m, 0.57 m and 0.23 m, respectively. Floors of the 1st and 2nd storeys at the main part of the building consist of timber beams with 0.085×0.19 m rectangular cross section, spaced at 0.4 m, with nailed timber boards on top and bottom, running in a direction perpendicular to the beam axis. The structural system of the 2nd storey ceiling, in the main part of the building, consists of rectangular 0.075×0.12 m timber beams spaced at 0.4 m. Floors of the 1st and 2nd storeys of the building's rectangular extension in the North-East direction, as well as the 2nd storey ceiling, are made of 0.14 m-high, double-T, iron beams, spaced at 0.5 m along the *Y* plan direction, having brick-arches spanning in the transverse direction and encased between the upper and lower flanges of successive iron beams.

3.2 Simulation and analyses details of the examined buildings

Investigation of the seismic response of the two examined buildings was pursued by simulating the buildings as three-dimensional finite element models (Figs. 5(b) and 6(b)) and by subjecting them to various earthquake scenarios. In all cases walls were idealized using four-nodded, thick, shell elements (6 d.o.f. per node). To simulate the construction practices of the 19th and 20th century, along the basement walls, above and below the basement windows, two 0.30 m thick zones of shell elements, accounting for solid brick lacing of the stone walls, were used. Vertical zones of solid, brick, shell elements, of the same thickness, were used on both sides of the basement windows and doors, simulating the construction practice that was used in order to form smooth surfaces at the edges of stone walls. Windows and doors ended in 0.30 m thick arches at the top, comprising solid bricks at the basement and voided bricks in the upper storeys, with a rise of 0.10 m at the center. Floors were modelled as a grid of linear elements that simulated the iron and timber beams, connected horizontally with shell elements that represented the brick arches, spanning between iron beams and the timber boards spaced orthogonally on top of the timber beams. In all cases, connection of the horizontal linear elements with the surrounding walls was achieved using contact springs, capable of transferring only axial and shear forces.

In all models, the response of the shell and the linear elements was considered elastic. The modulus of elasticity of stone and bricks was approximated as 500 times the value of the mean compressive strength of masonry, f_k (KADET 2014, cracked stiffness). In all building cases, the values of f_k considered for stone, solid bricks and voided bricks, were, 5.5 MPa, 4.0 MPa and 1.5 MPa, respectively. The modulus of elasticity of frame elements was taken equal to 150 GPa for the iron beams, 10 GPa for timber in the longitudinal direction of the beams and 1 GPa in the other two sectional directions. In all cases, self weight of the building was calculated according to the material density; this was taken equal to 25 kN/m^3, 18 kN/m^3 and 14 kN/m^3 for masonry made of stone, solid and voided bricks, respectively. Roof weight was taken equal to 1.5 kN/m^2 uniformly distributed along the area elements of the third storey roof in the case of the Papafeio Foundation and along the linear elements of the roof trusses of the 12th Primary School, according to their

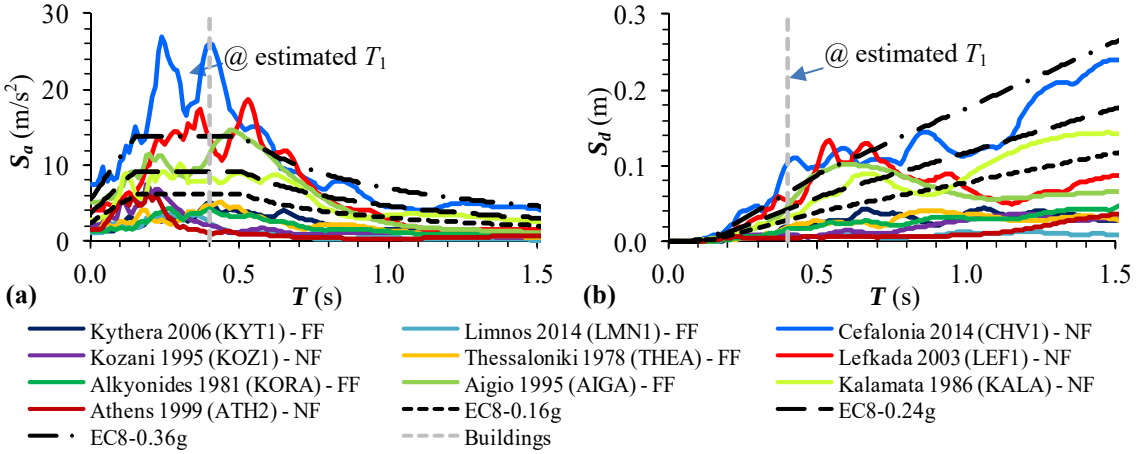

Fig. 7 Response spectra of the records used (ξ=5%): (a) absolute accelerations, (b) relative displacements. NF: Near Fault record, FF: Far Fault record

tributary area. Service loads were considered equal to 2.5 kN/m^2 for the roof and 3.5 kN/m^2 for the floors of the building. Masses considered in the dynamic analyses were automatically calculated by the program (=volume of element×material density).

To account for the effect of the ground motion parameters, a suite of ten earthquake records was used in conducting time-history dynamic analyses (available from www.itsak.gr). All acceleration records were derived from past strong earthquakes that have occurred in Greece between 1978 and 2014, which caused different types and extents of damage in numerous documented cases of URM buildings of the same type as those examined herein and of the same period of construction (19th and early 20th century). From among the ten earthquake records considered in the analyses, five were recorded in the near-fault zone (i.e., within 20 km from the rupture fault), whereas the other five datasets were recorded in sites with a distance from rupture fault ranging from 22 to 40 km. From among the three components recorded for each earthquake case (two horizontal and one vertical), the record used in dynamic analyses corresponds to the horizontal component with the maximum recorded absolute peak ground acceleration (PGA). These components were then applied separately, in each of the two principal directions in plan of the examined buildings. Fig. 7 plots the acceleration and displacement response spectra for the motions considered in the study, calculated with viscous damping ξ=5%.

3.3 Comparison between the results of the time-history and the static analyses

The relevance of the proposed static analysis procedure as a means to approximate the seismic response of URM buildings is first evaluated by comparing the pattern and intensity of the displacement demands throughout the structure with the displacement response envelopes obtained from dynamic time-history analysis for the two case studies considered. Different types of floors and roofs that provide different level of stiffness within the buildings' horizontal structural elements may be found in historical URM buildings. To investigate the influence of this variable two different versions of the Papafeio building model were subjected to time-history dynamic analysis for the case of the 1978 Thessaloniki earthquake, one where the stiffness contribution of

the horizontal structural elements (floors and roof) was neglected and one where full diaphragm action was assumed at the floor and roof levels (rigid diaphragms). The actual seismic response of the building lies within the response of these two extremes.

Fig. 8 plots displacement time-histories along the X and Y plan directions, for selected points of the plan of the Papafeio Foundation, derived from dynamic analyses of the two alternative building models, when subjected to seismic excitations parallel to X and Y directions, respectively. Each plot depicts a time interval of 1.5 s before and after the instant of maximization of the horizontal displacement of the control point in the same direction with the earthquake excitation. The time-histories of the displacements U_i, are normalized with respect to the peak horizontal displacement value occurring in the time-history at the examined locations, estimated from $U_{max}=\sqrt{(U_X^2+U_Y^2)}$, so as to investigate the influence of floor stiffness to the structure's response.

As depicted in Fig. 8, the degree of diaphragm stiffness has a crucial effect on the building's response. When floor stiffness is neglected (light blue and orange lines represent U_x and U_y, respectively), each of the control points of the building displaces not only parallel to the earthquake excitation but also in the orthogonal direction by a significant amount, which may exceed up to 50% of the magnitude of its principal displacement. This applies at the edges of the building and at walls whose plane of action is parallel to the direction of the earthquake excitation, whereas walls oriented orthogonal to the ground excitation deflect mainly in out-of-plane motion (e.g., Wall Y_2). Note that the waveform of developed displacements varies among the different

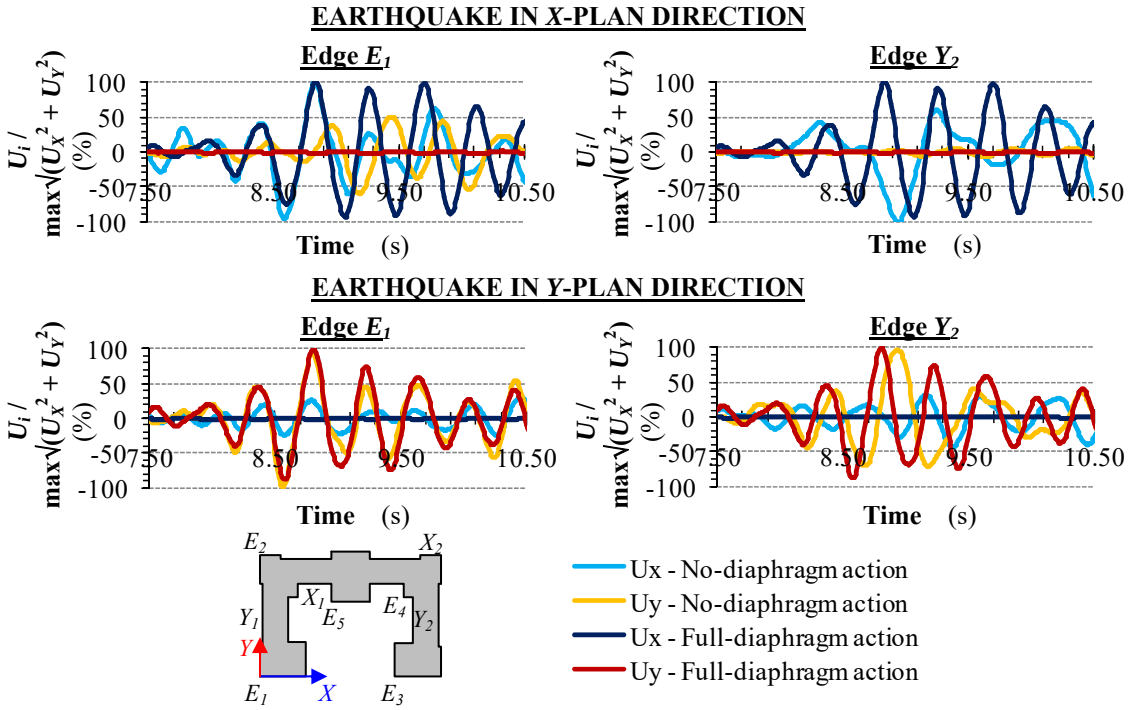

Fig. 8 Time-histories of the horizontal displacements in X and Y plan directions at selected points at the crest of the two alternative models of the Papafeio Foundation subjected to the 1978 Thessaloniki earthquake. In the case of earthquake action along X, values U_x and U_y are the responses obtained for the corresponding action. Similarly for action along Y

reference points of the building, indicating a differential movement within locations in the same horizontal level of the building owing to out-of-plane bending and torsional action. On the contrary, when full diaphragm action is considered, all reference points displace mainly parallel to the direction of the earthquake action, regardless of orientation of the walls to which they belong, with respect to the earthquake's direction (dark blue and red lines represent U_x and U_y, respectively).

Static analysis is conducted by applying the gravitational field in each of the structures along the principal direction of its geometry. Displacements obtained are normalized with respect to the corresponding displacement of the centroid of the building plan at the crest level of each examined building respectively: this point is considered in the remainder as the control node of the structure. After normalization the displacement profile of the entire structure has the significance of a 3-D shape function representing the sway response of the building. This is plotted by black dashed lines for various vertical lines through the structure in Figs. 9 and 10. For the shape function thus calculated, the excitation factor and mass participation coefficients are estimated from the following expressions

$$\Gamma_j = \left[\left(\sum_{i=1}^{N} m_i \cdot U_{i,j} \right) \Big/ \left(\sum_{i=1}^{N} m_i \cdot U_{i,j}^2 \right) \right] \tag{8a}$$

$$a_j = \left[\left(\sum_{i=1}^{N} m_i \cdot U_{i,j} \right)^2 \Big/ \left(\left(\sum_{i=1}^{N} m_i \right) \cdot \left(\sum_{i=1}^{N} m_i \cdot U_{i,j}^2 \right) \right) \right] \cdot 100 \tag{8b}$$

where, m_i are the finite element mode's nodal masses and $U_{i,j}$ is the pattern (shape) of nodal lateral displacements in the j-th plan direction (j=X or Y). Values are listed for the two parameters for the two buildings and for the different assumptions regarding the floor stiffness in Table 1. Note that mass participation is in the range of 45% with the corresponding excitation coefficient Γ in the range of 1.8.

In comparing the results between the proposed static and the time history analysis the focus is at peak response values, since those affect the design. Comparison is made with respect (a) the estimated peak displacement from the two approaches at a common point of reference, and (b) with respect to the profile of normalized lateral displacements, as that enables a comparison regarding the location of the critical regions in the structure (i.e., tendency for damage localization). Peak responses are listed in Table 1 for the same control node as that used for normalizing the static displacement pattern. Dynamic responses are correlated against the spectral values obtained for the response of the control node after multiplication with the excitation factor Γ. (Note that peak responses of the control node obtained from static analysis are the same in X and Y plan directions, as $T_{1,X}$=$T_{1,Y}$ (Eq. (2)).) Clearly the static demand estimate is conservative in the majority of the examples considered.

The relevance of the proposed static procedure in properly localizing the demands is illustrated through comparison of the normalized response shape envelopes plotted in Figs. 9 and 10 at selected control locations of the Papafeio Foundation and the 12th Primary School, respectively, when floor and roof stiffness has been neglected. The black dashed line in the following figures refers to the results of static analysis, whereas, colored lines represent the normalized displacement envelopes (i.e., peak values throughout the time history) developed by the structure at the respective locations. Each curve is normalized by the peak response of the control node for the

Table 1 Horizontal displacements of the control node of the examined buildings, obtained from Static and Time-History analyses

PAPAFEIO FUNDATION										
Analysis Type	Horizontal Displacement of Control Node (mm)									
	KYT1	LMN1	CHV1	KOZ1	THEA	LEF1	KORA	AIGA	KALA	ATH2
S_d	17.9	7.7	105.9	7.7	24.6	51.6	17.1	66.7	36.9	5.8
Static: $\Gamma \cdot S_d$	32.2	13.9	190.6	13.9	44.28	93.9	30.8	120.1	66.4	10.4
Time-History in X	21.0	8.3	87.9	10.3	20.2	74.4	18.6	64.8	55.5	6.5
Time-History in Y	18.2	7.9	74.7	8.7	18.5	63.0	16.4	63.5	41.7	6.1
12^{th} PRIMARY SCHOOL										
Analysis Type	Horizontal Displacement of Control Node (mm)									
	KYT1	LMN1	CHV1	KOZ1	THEA	LEF1	KORA	AIGA	KALA	ATH2
S_d	7.1	8.5	42.5	8.1	8.4	37.3	8.2	21.4	23.1	4.7
Static: $\Gamma \cdot S_d$	12.9	15.5	77.4	14.7	15.3	67.9	14.9	38.9	42.0	8.6
Time-History in X	11.6	13.7	50.8	11.3	14.9	38.3	13.7	34.2	37.0	4.3
Time-History in Y	9.8	9.8	70.7	8.8	12.2	35.4	10.1	28.4	30.1	5.5

ground motion considered, so that it represents the shape or pattern of lateral translation assumed by the structure at the critical instant. Note that the correlation between the result obtained from the proposed static analysis procedure and the associated time-history dynamic analyses improves when full diaphragm action is considered, especially at locations that were affected by out of plane action. In most of the cases depicted in Figs. 9 and 10, the normalized deformed shapes obtained from the proposed static analysis procedure envelopes the corresponding shapes resulting from dynamic analyses, whereas in the cases where the proposed static analysis seems to underestimate the deformed shape of the buildings, in fact, the actual horizontal deformations and interstorey drifts resulting from the static analysis are shown to be more conservative when the spectral displacement value is considered according with Eq. (4). For example, the horizontal displacement at roof level of control location Wall Y_1 of the Papafeio Foundation resulting from the Athens earthquake (dark red line in Fig. 9), the displacement calculated from time-history analysis is U_X=7.9·6.5=51.35 mm, whereas, the response obtained from static analysis is U_X=5.3·10.4=55.12 mm. Similarly, in the case of the 12^{th} Primary School subjected to earthquake excitation in its X plan direction, the Kozani earthquake seems to envelope the response deriving from the proposed static procedure along the Edge E_5 (purple line in Fig. 10). Yet, the actual roof displacement caused by the Kozani earthquake in this control location is U_X=1.5·11.3=16.9 mm, whereas, the proposed static analyses results in U_X=1.2·14.7=17.6 mm. Similar results also apply in all of the other graphs of Figs. 9 and 10, where the normalized deformed shapes deriving from application of the proposed static procedure seem to underestimate the building's actual seismic response. Therefore, peak responses of the two examined buildings obtained from the proposed static analysis procedure are always more conservative, than those obtained through dynamic analysis.

To appreciate the small level of mass participation occurring in URM structures, Table 2 also lists the values of a_j for the 12th Primary School, calculated using the normalized response envelopes at peak response obtained from time-history dynamic analyses. Values converge when the dynamic response envelope approaches that of the translational mode obtained from static

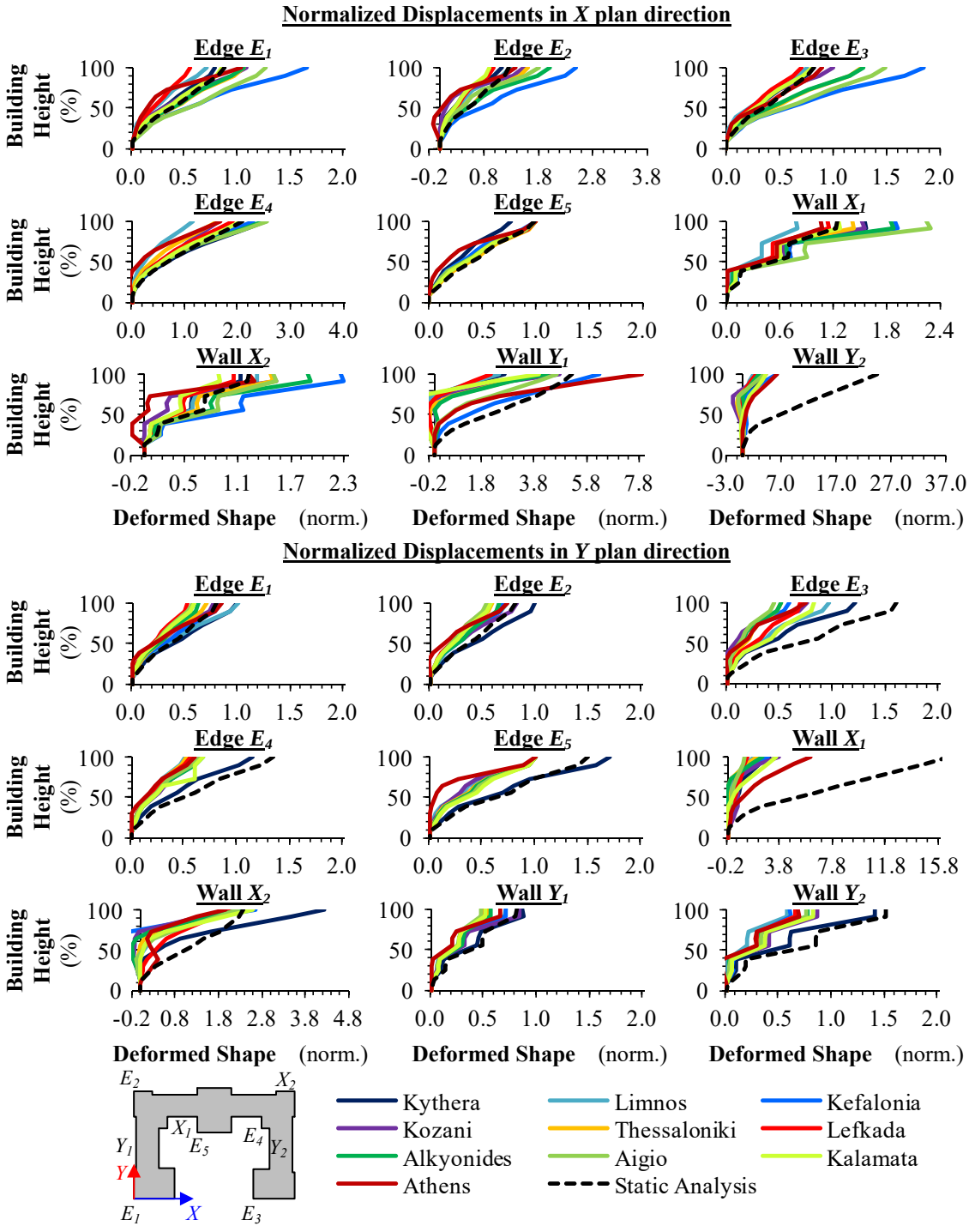

Fig. 9 Lateral displacement profiles at control locations of the Papafeio Foundation at the instant of the maximum roof displacement when the building is subjected to earthquake excitations in the same direction - No-diaphragm action considered

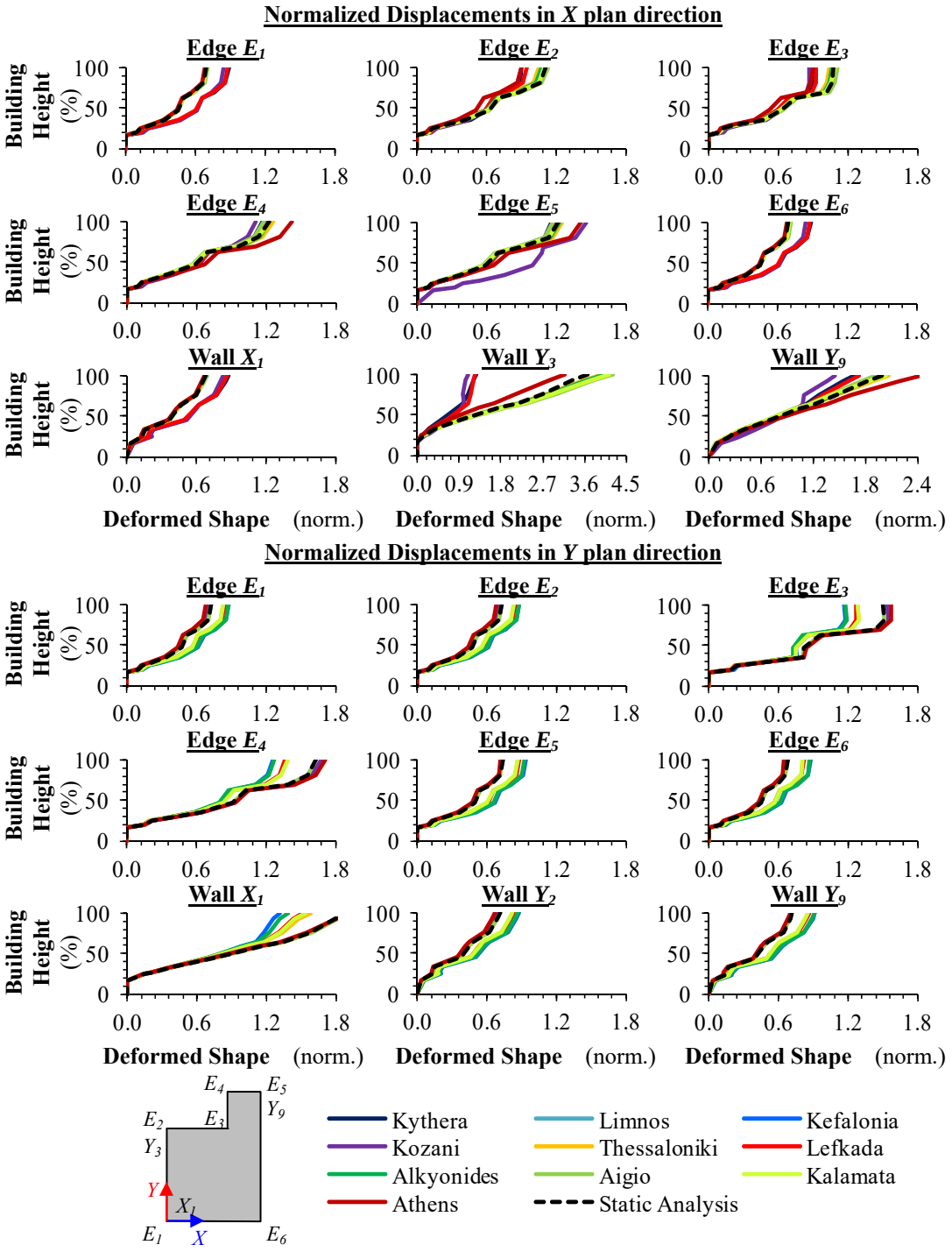

Fig. 10 Lateral displacement profiles at control locations of the 12th Primary School at the instant of the maximum roof displacement when the building is subjected to earthquake excitations in the same direction - No-diaphragm action considered

Table 2 Percentage of total mass that is activated at peak dynamic response of the 12th Primary School.

Analysis Type	Mass Participation coefficient, a (%)									
	KYT1	LMN1	CHV1	KOZ1	THEA	LEF1	KORA	AIGA	KALA	ATH2
Time-History in X	33.00	43.41	30.24	25.07	28.02	33.07	38.74	32.99	28.31	18.20
Time-History in Y	29.00	33.71	38.40	39.13	37.16	33.74	35.07	39.59	35.83	28.83

analysis (see Table 1). On the contrary, when the frequency content of the earthquake activates higher modes in the vibrating building (for example in Athens ground acceleration), a is significantly smaller that the corresponding value deriving from the proposed static analysis. In the latter cases, the normalized deformed shape exceeds locally the deformed shape obtained from static analysis, yet, the actual dynamic horizontal displacements are significantly smaller (see Table 1) from the static displacements, rendering the proposed static analysis procedure more conservative for seismic assessment even of these buildings.

Therefore, in terms of determination of the lateral displacement profiles, application of the rapid analysis procedure yields results of similar magnitude but more conservative that those of time-history dynamic analysis. Yet, application of the introduced rapid analysis procedure requires significantly less computational time and means (for example, in the case of the Papafeio Foundation the volume of produced output files in the case of time-history dynamic analyses ranged between 57 and 100 GB per record, requiring an execution time of about 18 to 40 h, whereas execution of the rapid analysis procedure in the same 3D finite element model required less than 2 min for excitation in each plan direction of the examined building model and the volume of the produced output files were in the range of 1 GB; note that the input file of the Papafeio building alone has a volume of 0.18 GB). Furthermore, the procedure is tailored to practical earthquake engineering as it can be used easily in conjunction with the design earthquake spectrum for the site considered. Thus, the proposed static analysis procedure is much simpler to process and handle than the time-history dynamic analysis procedure, especially in cases of massive structures, such as the monumental URM buildings, as the one studied herein; this renders the proposed approach a useful tool in the hands of practitioners in the field of seismic assessment.

4. Application example of rapid seismic assessment of a historical monumental URM building

To demonstrate the application process of the methodology for URM buildings, the assessment details of the second case study are listed here. The seismic hazard defined as per the EN1998-1 (2004) taking into consideration the building's site characteristics are, γ_I=1.3, a_{gR}=0.16 g in the case of Thessaloniki, S=1.15 for soil type C. Material properties used in this procedure were selected in accordance with standards of the time of construction, as well as from limited in-situ testing, as f_m=1.50 MPa, f_{vm0}=0.10 MPa, f_b=20.0 MPa, f_{wt}=0.30 MPa for solid bricks and stones. Also considered, according to EC8-3 (2005), is CF=1.35.

The fundamental translational period of vibration in both plan directions, T_1, is estimated from Eq. (2) as $T_1=0.050 \cdot H^{3/4}=0.050 \cdot 11.90^{3/4}=0.32$ $s < T_C$ (=0.50 s). From Eq. (3) the acceleration response of the ESDOF is $S_a(T_1)=\gamma_I \cdot a_{gR} \cdot S \cdot 2.5=5.9$ m/s^2. Thus the target roof displacement at the

centroid of the building is $S_d(T_C)=S_a(T_1)\cdot T_C^2/40=15$ mm (Eq. (3)). The control node displacement is therefore estimated as $\Gamma\cdot 15=27.3$ mm. Local displacements are obtained by multiplying $\Gamma\cdot S_d$ with the normalized deformed shape of the building.

With regards to in-plane wall deformations in the absence of stiff diaphragms H_o in Eq. (5) is taken equal to the storey height (i.e., $H_o=\{4.90, 4.40\}$ m with regards to the 2nd storey and the 1st storey. In the case of the 1st storey X_1 external wall (Fig. 6(e)-(g)), where $L=L'=4.93$ m and N, deriving from vertical loading of the building according to the seismic loading combination G+0.5Q, equals to 365.93 kN and $f_d=f_m/CF_m=1.50/1.35=1.11$ MPa, leads to: $0.065\cdot f_d\cdot L'\cdot t=0.065\cdot(1.11\cdot 10^3)\cdot 4.93\cdot 0.46=163.62$ kN and $0.4\cdot N=0.4\cdot 365.93=146.37$ kN. Therefore, $V_s=146.37$ kN. Furthermore, $V_f=[(L\cdot N)/(2\cdot H_o)]\cdot[1-1.15\cdot N/(L\cdot t\cdot f_d)]=[(4.93\cdot 365.93)/(2\cdot 4.40)]\cdot[1-1.15\cdot 365.93/(4.93\cdot 0.46\cdot 20.0\cdot 10^3)]=169.64$ kN. The comparison between V_f with V_s leads to the conclusion that premature failure of the wall, due to exhaustion of its shear strength, will occur. Yet, V, as calculated according to the static analysis, equals to 111.24 kN, which is smaller than V_s, therefore the wall will remain intact. By following the same procedure for all walls, it is found that no failure is anticipated. By comparing the values of θ_{in} developed in the building's walls, as those result from the proposed static analysis procedure, with the limiting values due to flexural or shear wall response (Eq. (7)), it is anticipated that the building will respond elastically (i.e., $q<1$, so there is no global ductility demanded by the building).

Finally, damage patterns developed due to out-of-plane wall deformation are investigated. In the case of the 1st storey X_1 external wall, when out-of-plane bending parallel to the wall's length is considered, $\theta_{u,1} = 0.003\cdot(4.93/2)/0.46 = 1.61\%$ and $\theta_{R,u} = 0.46/(4.93/2) = 18.66\%$, $M_y = (0.30\cdot 1000)\cdot(4.90\cdot 0.46^2)/6 = 51.8$ kNm, $F_{Rd} = 5.9\cdot 0.46\cdot 18\cdot(4.93\cdot 4.90-1.25) = 1119.1$ kN and $M_{Rd} = 1119.1\cdot(4.90/2)/2 = 1370.9$ kNm. Therefore, $\theta_{u,2} = 18.66\%\cdot(1-51.8/1370.9) = 17.95\%$ and $\theta_u = \min\{\theta_{u,1}, \theta_{u,2}\} = 1.61\%$. Similar calculations when out-of-plane bending vertically to the wall's length is considered, where $M_y = 115.0$ kNm due to the effect of $N = 365.93$ kN, resulted to the same value of θ_u. According to the results of the static analysis, θ_{out} equals to less than 0.20% in all walls of the building. Where the value of 0.20% is reached the likelihood of cracking is great; this is near the Performance Limit State of Damage Limitation according to EN1998-3 (2005).

Locations where drift ratio values are within ±25% of the assumed cracking limit are identified in yellow in the envelope of the building in Fig. 11 These results are of the seismic assessment procedure are also verified by the actual seismic response of the building during the 1978 Thessaloniki earthquake (Peak Ground Acceleration=0.15 g), where minimal cracking was

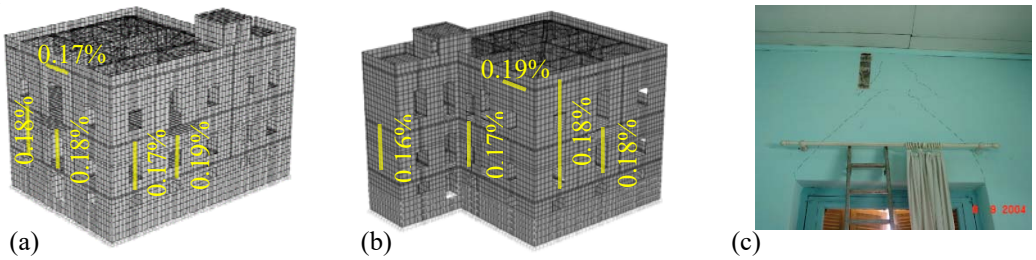

(a) (b) (c)

Fig. 11 (a)-(b) Anticipated damages at the 12th Primary School resulting from the design earthquake (a_g=0.16 g): vertical lines correspond to in-plane wall response, horizontal lines correspond to out-of-plane wall response, (c) Cracks over the door of the 2nd storey external wall X_2 developed after the 1978 Thessaloniki earthquake (as illustrated in Fig. 11(a) in the same location θ_{out} was estimated equal to 0.17%)

reported in lintels above windows without other significant damage and the school continued its operation.

5. Conclusions

This paper investigates the seismic response of historical and monumental unreinforced masonry buildings built during the post-renaissance era. Buildings of this category possess special dynamic characteristics, deriving from the principals governing their architectural design, which lead to a certain pattern of response during an earthquake excitation. Among them, monumental buildings are especially vulnerable as due to their shape in plan often develop torsional phenomena during a seismic excitation, capable of causing important differential displacements along their structural system and therefore damage localization in their remotest locations. Given the historical value of heritage and monumental buildings, which in many cases are inseparably connected with political, economical or cultural national milestones, seismic assessment of them is an essential step towards identifying potential locations of damage and towards selecting the appropriate retrofit strategy that will secure the integrity of those structures as well as the preservation of their unique historic and architectural characteristics.

In this framework, the fast seismic procedure for unreinforced masonry buildings, which has recently been developed by the authors (Pardalopoulos *et al*. 2015), has been applied to two neoclassical buildings of Thessaloniki, Greece and results have been evaluated to assess the extent of anticipated damage. It was shown that the assessment procedure yielded results of equivalent accuracy to detailed time-history dynamic analysis based assessment procedures, as well as to the actual seismic response of the examined buildings. Yet, the introduced procedure required significantly shorter computational time and effort while being compatible with the use of design spectra for definition of the seismic hazard, and produced significantly smaller volume of output files, which renders it ideal for practical use, especially in the case of massive structures such as state heritage buildings, where, even when powerful computational means are utilized, seismic assessment can be an especially demanding task.

Acknowledgments

This research was conducted partly at the University of Cyprus, where the first author was Visiting Researcher, while a Postdoctoral Fellow at the Institute of Engineering Seismology and Earthquake Engineering and it was funded by the Greek State Scholarships Foundation in the framework of the Short Terms scholarship program, under the 2013-ΠΕ2-SHORT TERMS-18496 contract.

References

ATC-40 (1996), *Seismic evaluation and retrofit of concrete buildings*, Applied Technical Council - California Seismic Safety Commission, Report No. SSC 96-01 (two volumes), Redwood City, CA, USA.

Borzi, B., Crowley, H. and Pinho, R. (2008), "Simplified pushover-based earthquake loss assessment (SP-BELA) method for masonry buildings", *Int. J. Architect. Herit.*, **2**(4), 353-376.

Bracchi, S., Rota, M., Penna, A. and Magenes, G. (2015), "Consideration of modelling uncertainties in the seismic assessment of masonry buildings by equivalent-frame approach", *Bull. Earthq. Eng.*, **13**(11), 3423-3448.

D' Ayala, D. and Lagomarsino, S. (2015), "Performance-based assessment of cultural heritage assets: outcomes of the European FP7 PERPETUATE project", *Bull. Earthq. Eng.*, **13**(1), 5-12.

EN 1998-1 (2004), *Eurocode 8 - Design of Structures for Earthquake Resistance-Part 1: General Rules, Seismic Actions and Rules for Buildings*, European Committee for Standardization, Brussels.

EN 1998-3 (2005), *Eurocode 8 - Design of Structures for Earthquake Resistance - Part 3: Assessment and retrofitting of Buildings*, Brussels: European Committee for Standardization.

Clough, R.W. and Penzien, J. (1976), *Dynamics of Structures*, 1st Edition, Mc Graw Hill, New York, USA.

Giresini, L., Fragiacomo, M. and Lourenco, P.B. (2015), "Comparison between rocking analysis and kinematic analysis for the dynamic out-of-plane behavior of masonry walls", *Earthq. Eng. Struct. Dyn.*, **44**(13), 2359-2376

Griffith, M., Magenes, G., Melis, G. and Picchi, L. (2003), "Evaluation of out-of-plane stability of unreinforced masonry walls subjected to seismic excitation", *J. Earthq. Eng.*, **7**(S1), 141-169.

ICOMOS (1964), "International charter for the conservation and restoration of monuments and sites, decisions and resolutions, document 1", *2nd International Congress of the Architects and Technicians of Historic Monuments*, Venice.

Illampas, R., Charmpis, D.C. and Ioannou, I. (2014), "Laboratory testing and finite element simulation of the structural response of an adobe masonry building under horizontal loading", *Eng. Struct.*, **80**, 362-376.

KADET (2014), *Hellenic code for assessment and structural interventions in masonry buildings*, Organization for Seismic Design and Earthquake Protection, Athens, Greece.

Kouris, L.A.S. and Kappos, A.J. (2015), "Fragility curves and loss estimation for traditional timber-framed masonry buildings in Lefkas, Greece", *Seismic Assessment, Behavior and Retrofit of Heritage Buildings and Monuments, Computational Methods in Applied Sciences*, **37**, 199-233

Lagomarsino, S., Penna, A., Galasco, A. and Cattari, S. (2013), "TREMURI program: an equivalent frame model for the nonlinear seismic analysis of masonry buildings", *Eng. Struct.*, **56**, 1787-1799

Muto, K., Takahasi, R., Aida, I., Ando, N., Hisada, T., Nakagawa, K. and Osawa, Y. (1960), "Nonlinear response analyzers and application to earthquake resistant design", *Proceedings, 2nd World Conference on Earthquake Engineering*, Japan.

Newmark, N.M., Blume, J.A. and Kapur, K.K. (1973), "Seismic design spectra for nuclear power plants", *Journal of the Power Division,* American Society of Civil Engineers, **99**, No PO2, New York, NY, USA.

Pantazopoulou, S.J. (2013), "State of the art report for the analysis methods for unreinforced masonry heritage structures and monuments", *European Center for Preparedness and Forecasting of Earthquakes*, http://www.ecpfe.oasp.gr/en/node/89.

Pardalopoulos, S.I., Pantazopoulou, S.J. and Kontari, M.Th. (2015), "Rapid seismic assessment procedure of masonry buildings with historic value", *Seismic Assess., Behav. Retrofit Herit. Build. Monuments, Comput. Meth. Appl. Sci.*, **37**, 113-137.

Pardalopoulos, S.I. and Pantazopoulou, S.J. (2015), "Vulnerability of torsionally sensitive historical buildings under seismic loads", *5th ECCOMAS Thematic Conference on Computational Methods in Structural Dynamics and Earthquake Engineering - COMPDYN 2015*, Crete Island, Greece.

Psycharis, I.N., Fragiadakis, M. and Stefanou, I. (2013), "Seismic reliability assessment of classical columns subjected to near-fault ground motions", *Earthq. Eng. Struct. Dyn.*, **42**(14), 2061-2079.

Roca, P., Cervera, M., Gariup, G. and Pela, L. (2010), "Structural analysis of masonry historical constructions. Classical and advanced approaches", *Arch. Comput. Meth. Eng.*, **17**(3), 299-325.